CHAPTER IV
RESULTS AND DISCUSSION

4.1 Characterization of Organomodified Bentonite and Montmorillonite

Fig. 4.1 and Fig. 4.2 show the X-ray diffraction patterns of Na-BN and Na-MMT and theirs alkylammonium derivatives. The peaks correspond to the (001) reflections of the clay. The d_{001} peak of pristine Na-BN at $2\theta=5.92°$ corresponds to 1.49 nm (Fig. 4.1a) basal spacing. The d_{001} peaks of organomodified bentonite (Fig. 4.1b, c, d, and e) are observed at lower angle than that of pristine Na-BN, these indicate the ammonium ions intercalate into the silicate layers and expand the basal spacing.

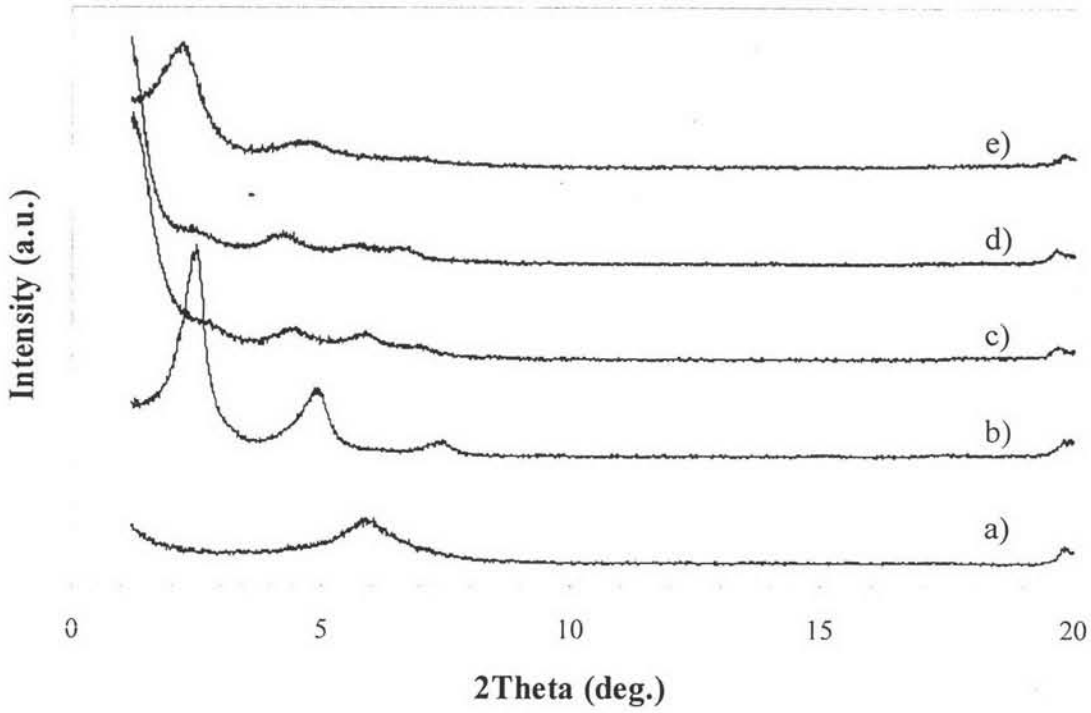

Figure 4.1 The WAXD patterns of organomodified bentonite: (a) Na-BN, (b) DTDM-B, (c) DCEM-B, (d) DOEM-B, (e) DOAM-B.

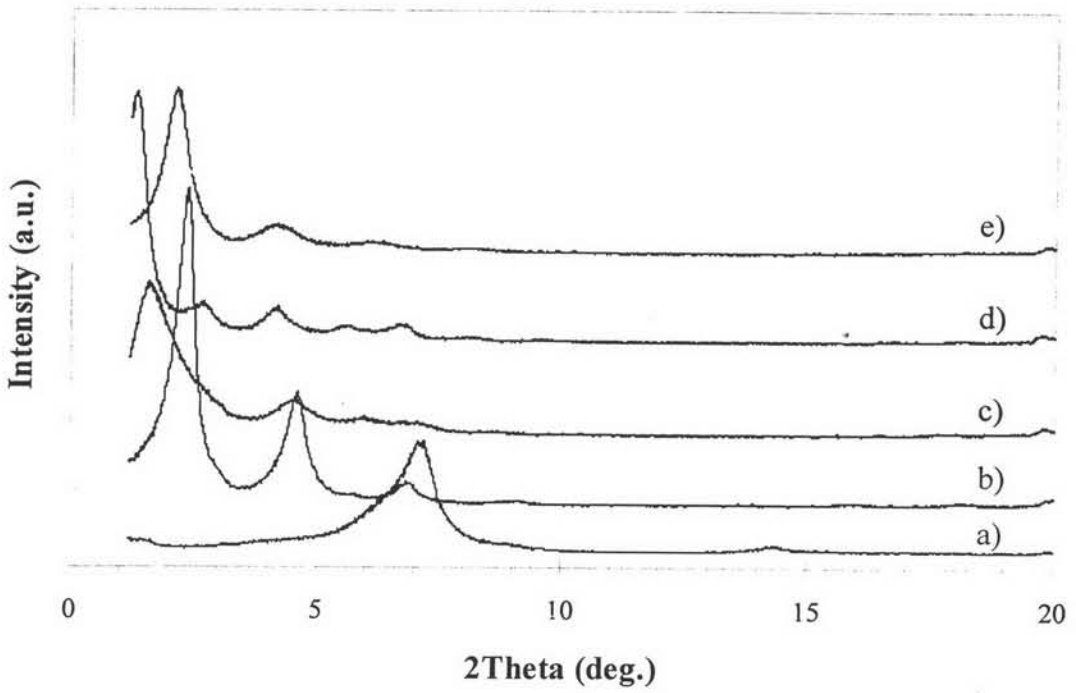

Figure 4.2 The WAXD patterns of organomodified montmorillonite: (a) Na-MMT, (b) DTDM-M, (c) DCEM-M, (d) DOEM-M, (e) DOAM-M.

From Fig. 4.1, it can be seen that the four types organomodified bentonite have different basal spacing (Table 4.1) which has the same tendency as organomodified montmorillonite (Table 4.1). The basal spacing of DTDM-B (Fig. 4.lb) having two long chain carbons shows two characteristic peak of silicate layer which are 3.51 nm for maximum and 1.80 nm for minimum basal spacing. This is due to the different arrangements of two chains in the interlayer space of silicate layer, as reported by Williams-Daryn and Thomas (2002). A larger interlayer separation of DCEM-B (6.84 nm as show in Fig. 4.lc) compared to that of DTDM-B might be due to the bulky functional groups like ethyl alcohol and ester, which correspond to paraffin-type bilayer orientation of organic molecules. While the basal spacing of DOEM-B (Fig. 4.ld) and DOAM-B (Fig. 4.le) having different bulky functional groups (as show in Table 4.1) are 7.06 and 3.99 nm, which correspond to paraffin-type bilayer and monolayer orientation of organic molecules, respectively. It is noted that DOAM contains amino groups that are capable of making H-bond

between chains. This induce better packing and thus showing lower expanded basal spacing than DOEM-B which possesses ester groups acting as steric hindrances.

Table 4.1 Characteristics of the organomodified clay

		Sample name				
		Clay	DTDM	DCEM	DOEM	DOAM
Organo-surfactant						
Main chain carbon number		-	18	18	20	20
Functional group		-	-	Hydroxy Ester	Hydroxy Ester	Hydroxy Amide
Basal spacing (nm)	Na-BN	1.49	3.51	6.84	7.06	3.99
	Na-MMT	1.23	3.71	5.73	6.59	4.11

Table 4.2 Thermal behaviors of organomodified clay

Sample name	Mass loss H_2O (wt %)	Mass Surfactant		Char residual (wt %)	T_d (^{0}C)	T_i (^{0}C)	T_f (^{0}C)
		wt %	mole				
Na-BN	9.9	-	-	-	-	-	-
DTDM-B	0.8	34.1	0.06	62.6	303.3	252.2	428.9
DCEM-B	1.3	32.8	0.04	61.9	340.4	249.2	372.8
DOEM-B	1.6	36.1	0.05	57.9	352.4	261.6	374.4
DOAM-B	0.8	30.4	0.04	66.5	396.3	238.6	530.2
Na-MMT	10.2	-	-	-	-	-	-
DTDM-M	1.3	51.8	0.09	43.1	318.7	257.5	441.3
DCEM-M	1.0	50.2	0.07	48.2	344.5	270.5	370.7
DOEM-M	0.4	49.4	0.06	41.4	346.0	250.3	366.7
DOAM-M	1.0	48.5	0.06	49.6	393.1	287.6	457.3

The thermal analysis of Na-BN and Na-MMT and theirs alkylammonium derivatives are represented in Table 4.2. On the organomodified bentonite or montmorillonite, the weight-loss of water desorption was around 1% and very large amount of weight-loss was shown at the temperature range of 250–450°C, which was related to the thermal decomposition of the organo-surfactant. The weight-loss of organomodified montmorillonite was larger than that of organomodified bentonite, which means that the amount of the exchanged organo-surfactant in the montmorillonite interlayer was larger than that of the exchanged organo-surfactant in the bentonite interlayer.

The presence of organo-surfactant on clay particles were confirmed by FTIR. FT-IR spectra were recorded in the region of 400-4000 cm^{-1}. Fig. 4.3 shows the IR spectra of Na-BN and Na-MMT and theirs alkylammonium derivatives. A pair of strong bands near 2850 and 2930 cm^{-1} at each spectrum can be assigned to the

symmetric and asymmetric stretching vibrations of the methylene group (υCH_2) of the guest molecules. Na-BN and Na-MMT were organomodified with DCEM and DOEM, including the ester group, a strong absorption band at 1740 cm^{-1} due to the stretching vibration of the carbonyl (-C=O-) group was observed. In the case of Na-BN and Na-MMT organomodified with DOAM, including the amide group, a strong absorption band at 1640 cm^{-1} due to the stretching vibration of the carbonyl (-C=O-) group and absorption band at 1540 cm^{-1} due to the (-NH-) stretching vibration were observed, supporting the intercalation of surfactant molecules between the silicate layers. The characteristic band in the range of 3200-3600 cm^{-1} belonged to hydroxyl group on the silicate layer which also observed in preparation montmorillonite with various chemical surface modification methods by Yang *et al.* (1999).

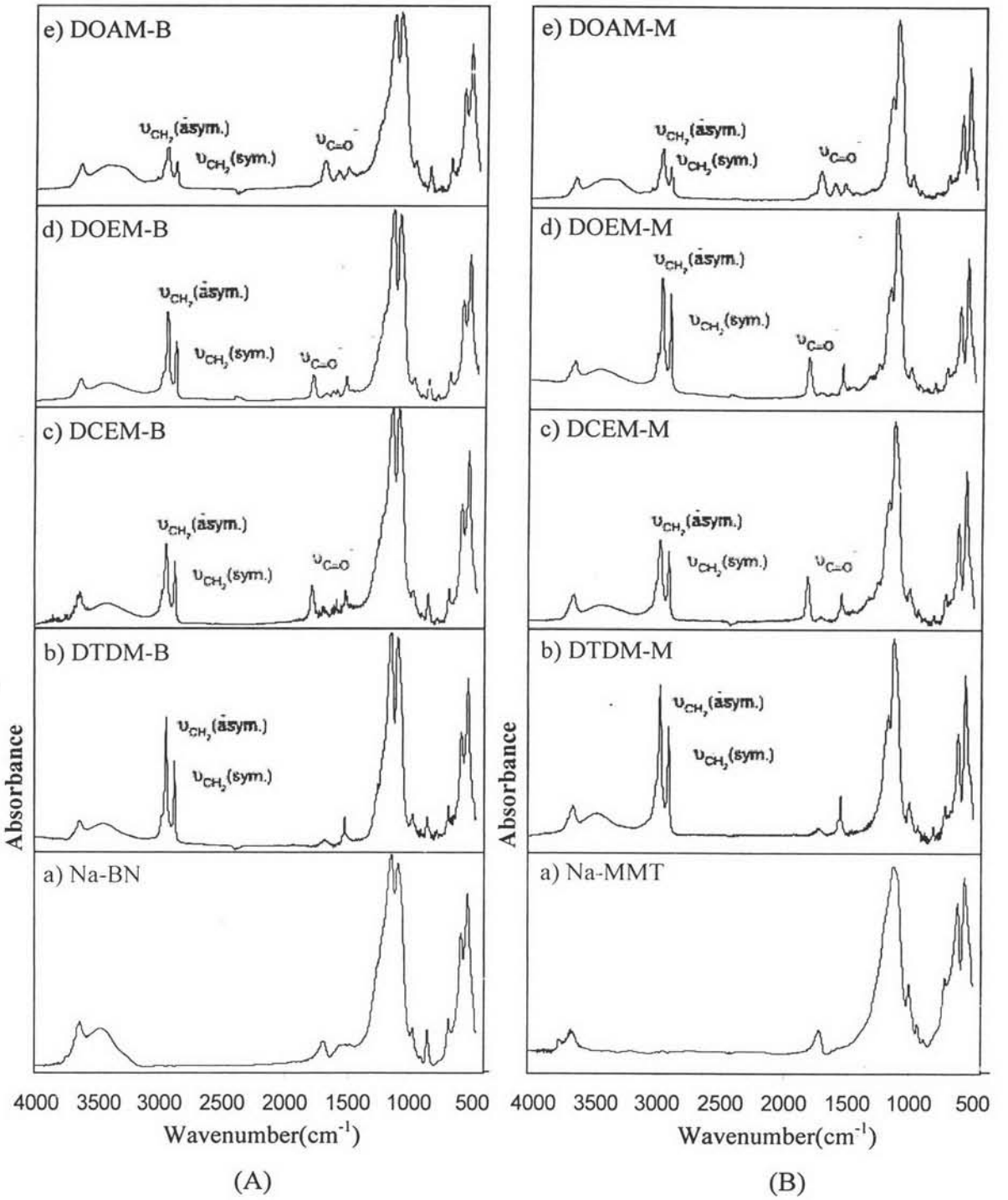

Figure 4.3 Infrared spectra of pristine clays and theirs quarternary alkylammonium derivatives: (A) organomodified bentonite, (B) organomodified montmorillonite.

4.2 Selection of Compatibilizer Loading

The compatibilized surlyn with three different weight percentage (3%, 6% and 9%) were melt mixed with 3% DTDM-B organoclay and PP to form nanocomposites. The X-ray diffraction patterns of clays (DTDM-B) and composites with different surlyn loading are showed in Fig. 4.4. The d_{001} peak of silicate clay layer of DTDM-B organoclay displays its characteristic peak at 3.51 nm basal spacing. XRD pattern of PP/Surlyn composite shows a little increased basal spacing (3.79 nm.) from pristine DTDM-B, indicating the silicate layer dispersed in the polymer matrix retained the stacked structure of pristine DTDM-B and also an immiscible dispersion of the clay in PP matrix. When the compatibilizer surlyn with different loading is introduced, the characteristic peak of DTDM-B disappears in the PP/Surlyn/DTDM-B composites. The absence of the d_{001} peak in XRD pattern suggests that the clay has a nearly exfoliated dispersion in the polymer matrix.

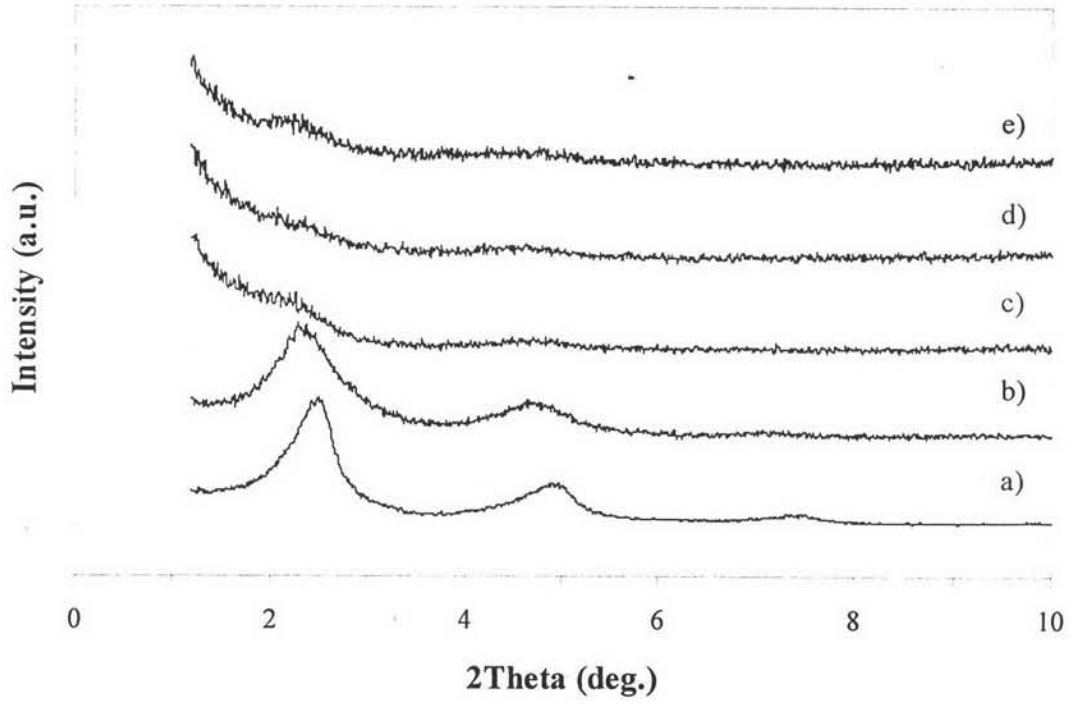

Figure 4.4 The WAXD patterns for (a) DTDM-B, (b) PP/ DTDM-B, (c) PP/ DTDM-B/ 3%Surlyn, (d) PP/ DTDM-B/ 6%Surlyn, (e) PP/ DTDM-B/ 9%Surlyn.

Table 4.3 Effect of compatibilizer loading on mechanical properties

Composition	Young's modulus (MPa)	Tensile strength (MPa)	% Strain at break (%)	Impact strength (kJ/m^2)
PP	1627.41	33.22 ± 0.2	270.33	2.9 ± 0.3
PP + 3%DTDM-B	1251.24	31.37 ± 0.9	15.64	2.3 ± 0.2
PP + 3%DTDM-B + 3%Surlyn	1659.04	32.06 ± 0.9	88.74	2.5 ± 0.4
PP + 3%DTDM-B + 6%Surlyn	1848.63	33.49 ± 0.3	62.76	3.0 ± 0.4
PP + 3%DTDM-B + 9%Surlyn	1831.68	32.09 ± 0.9	78.30	2.6 ± 0.4

Table 4.3 shows mechanical properties of composites and virgin PP. The compatibilized PP/clay nanocomposites exhibited improved young's modulus, tensile strength, strain at break and impact strength in comparison to the uncompatibilized one. However, modulus, tensile strength and impact strength values are slight increased for 6% Surlyn addition, which is decreased for 9%. These improved modulus, tensile and impact strength of compatibilized nanocomposites might be due to the effects on the polymer-clay interface. Addition of compatibilizer facilitates easier intercalation of the polymer within the clay galleries. The miscibility of the Surlyn ionomer with polar groups of the nanoparticles and the PP matrix mediate between the surface chemistry of the polymer and the clay at the interphase, which significantly increases in the modulus as observed for other compatibilized systems. However, the decreased strength for higher Surlyn content is attributed to the increased amount of low molecular weight oligomer fraction of the Surlyn ionomer.

The actual clay content and thermal stability of composites, as shows in Table 4.4, was found by TGA analysis. The clay percentage by weight was around 2% in the sample of 3 wt% clay was added during the nanocomposites preparation. The thermal decomposition of the compatibilized nanocomposites was observed at higher temperature than the uncompatibilized nanocomposites one and virgin PP. The 6% Surlyn addition in nanocomposites shows the highest thermal stability. When the Surlyn content is increased as 9 wt%, the thermal stability is more or less steady.

This shows the same tendency with the mechanical properties. Based on above analyses, 6 wt% Surlyn was chosen as a compatibilizer loading in the preparing nanocomposites for evaluating the effect of the surfactant structure on organoclay exfoliation.

Table 4.4 Effect of compatibilizer loading on thermal properties

Composition	TGA			
	Clay content (wt %)	T_d (^{0}C)	T_i (^{0}C)	T_f (^{0}C)
PP	-	455.8	432.1	468.4
PP + 3%DTDM-B	2.4	432.4	427.4	434.8
PP + 3%DTDM-B + 3%Surlyn	1.6	459.8	434.9	468.5
PP + 3%DTDM-B + 6%Surlyn	2.1	460.1	435.6	471.1
PP + 3%DTDM-B + 9%Surlyn	1.8	459.0	437.1	472.8

4.3 Characterization of Nanocomposites

4.3.1 Structure Analysis of Nanocomposites

Fig. 4.5 and Fig. 4.6 show the SAX patterns of nanocomposites formed from the different type of Na-BN and Na-MMT. The peaks correspond to the (001) reflections of the clay. It can not be observed in the XRD patterns of both modified Na-BN and Na-MMT composites modified with cationic surfactant having functional group suggesting that the silicate clay layers have a nearly exfoliated dispersion in the polymer matrix (Alexandre and Dubois, 2000). However, the XRD pattern of nanocomposites modified with DTDM exhibits a basal spacing increasing from 3.51 nm for modified bentonite to 4.25 nm for its nanocomposite (Fig. 4.5a). For PP/DTDM-M nanocomposite (Fig. 4.6a), it shows a basal spacing increasing from 3.71 nm for Na-MMT modified with DTDM to 4.09 nm for its nanocomposite. The absence of the d_{001} peak and increase of basal spacing are due to the PP and surlyn intercalation between the silicate clay layer.

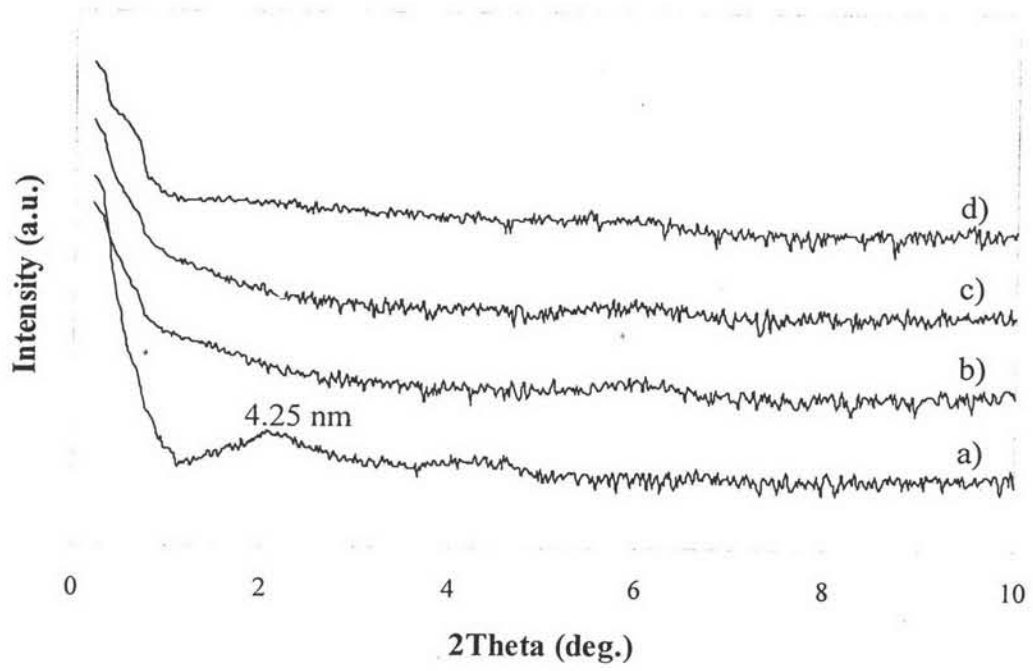

Figure 4.5 The SAX patterns for (a) PP/Surlyn/DTDM-B, (b) PP/Surlyn/DCEM-B, (c) PP/Surlyn/DOEM-B, (d) PP/Surlyn/DOAM-B.

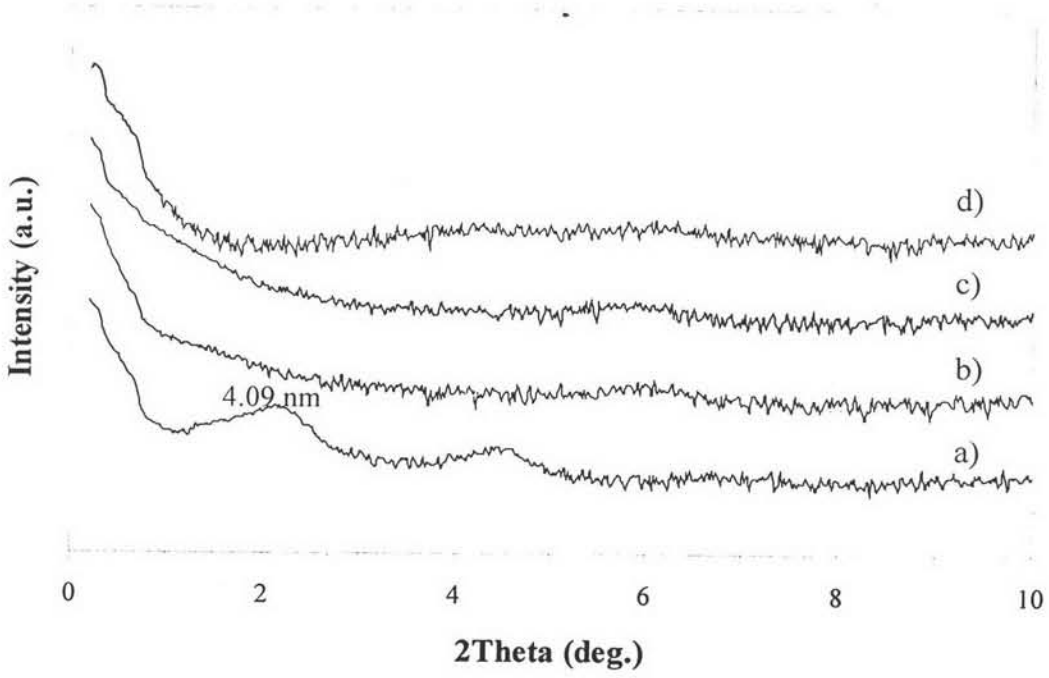

Figure 4.6 The SAX patterns for (a) PP/Surlyn/DTDM-M, (b) PP/Surlyn/DCEM-M, (c) PP/Surlyn/DOEM-M, (d) PP/Surlyn/DOAM-M.

4.3.2 Melting and Crystallization Behavior

Melting and crystallization behavior of PP and nanocomposites formed are reported in Fig. 4.7. The melting point and crystallization characteristics of the nanocomposites are not changed when compared to the virgin PP. This might be due to the nanoscale fillers do not affect the crystallite size of the base polymer. The characteristic peaks of PP crystal phase were analyzed by XRD with the 2θ range of 10-30°, as shown in Fig.4.8. and 4.9. Pure PP shows five prominent which correspond to monoclinic α crystalline phase: α_1 belongs to the (110) reflection, α_2 to the (040) reflection, α_3 to the (130) reflection and α_4 the (111) and (041) reflections. These reflection correspond to 2θ=14.04, 16.86, 18.50, 21.08 and 21.72°, respectively. The result indicated that there is no observed difference between PP and nanocomposites formed. The presence of organomodified bentonite and mont-morillonte does not affect the crystal structure of PP matrix in this case, as already observed for other PP/ clay nanocomposites by Ding *et al.* (2004) and Ramos Filho *et al.* (2005).

The melting enthalpy (ΔHm) value of pure PP and nanocomposites with variuos modifying agents, obtained via DSC was also given in Table 4.5. The melting enthalpy (ΔHm) of nanocomposites modified with organo-surfactant having functional group show slightly increase when compared to the nanocomposites modified with DTDM.

Table 4.5 Melting and crystallization behavior of PP and nanocomposites

Composition	T_c (^{0}C)	T_m (^{0}C)	ΔHm	% Crystallinity
PP	110.8	161.7	66.46	31.80
PP + Surlyn + DTDM-B	108.9	160.7	63.05	32.83
PP + Surlyn + DCEM-B	109.6	157.7	65.56	34.17
PP + Surlyn + DOEM-B	110.8	158.7	61.01	31.87
PP + Surlyn + DOAM-B	109.5	158.2	63.99	33.39
PP + Surlyn + DTDM-M	108.1	158.8	63.34	33.01
PP + Surlyn + DCEM-M	109.1	158.0	65.22	33.77
PP + Surlyn + DOEM-M	108.1	158.5	64.02	33.26
PP + Surlyn + DOAM-M	108.1	158.9	66.73	34.59

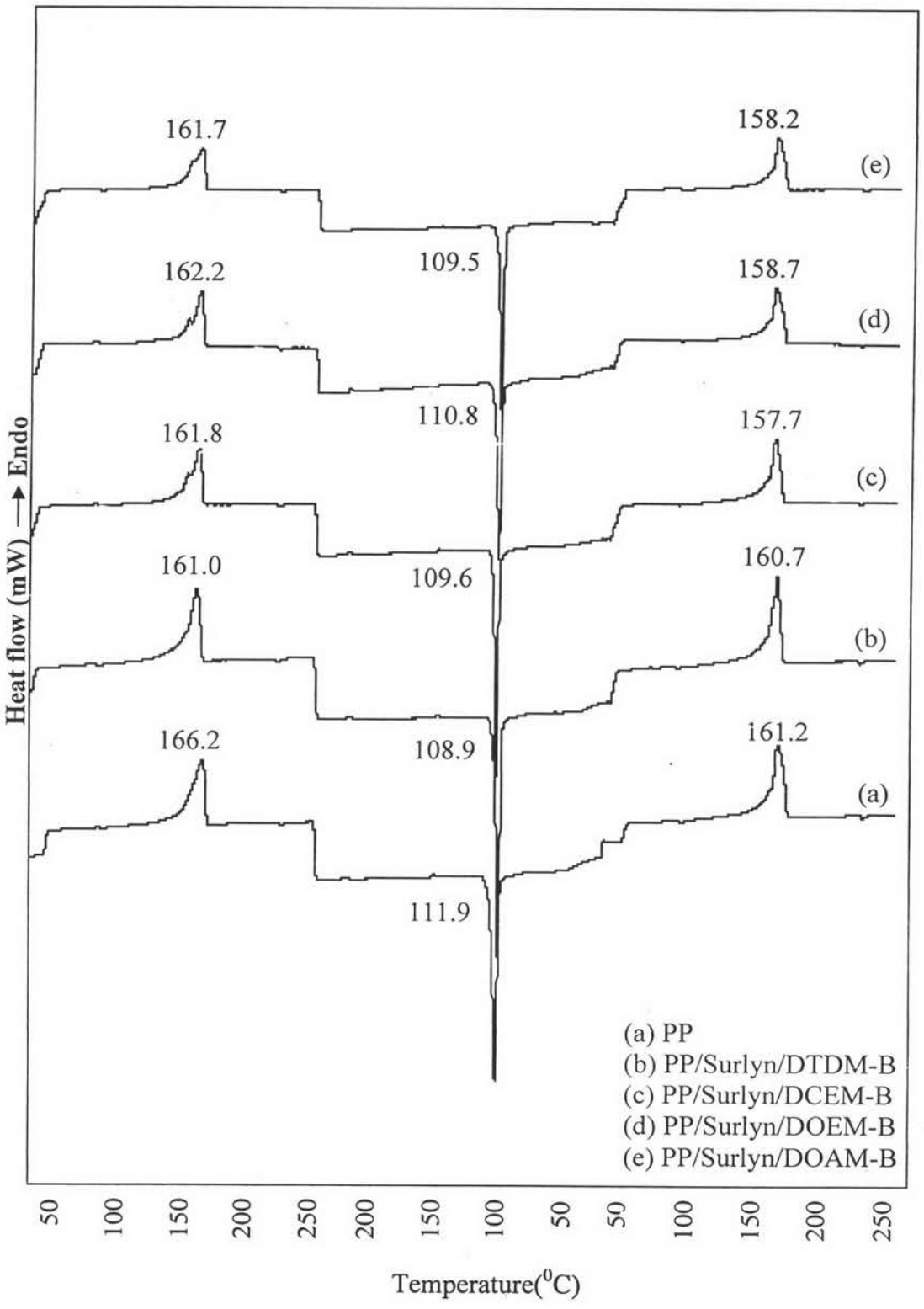
161.7
158.2
(e)
109.5
162.2
158.7
(d)
110.8
161.8
157.7
(c)
109.6
161.0
160.7
(b)
108.9
166.2
161.2
(a)
111.9
(a) PP
(b) PP/Surlyn/DTDM-B
(c) PP/Surlyn/DCEM-B
(d) PP/Surlyn/DOEM-B
(e) PP/Surlyn/DOAM-B
Heat flow (mW) → Endo
50 100 150 200 250 200 150 100 50 50 100 150 200 250
Temperature(°C)

(A)

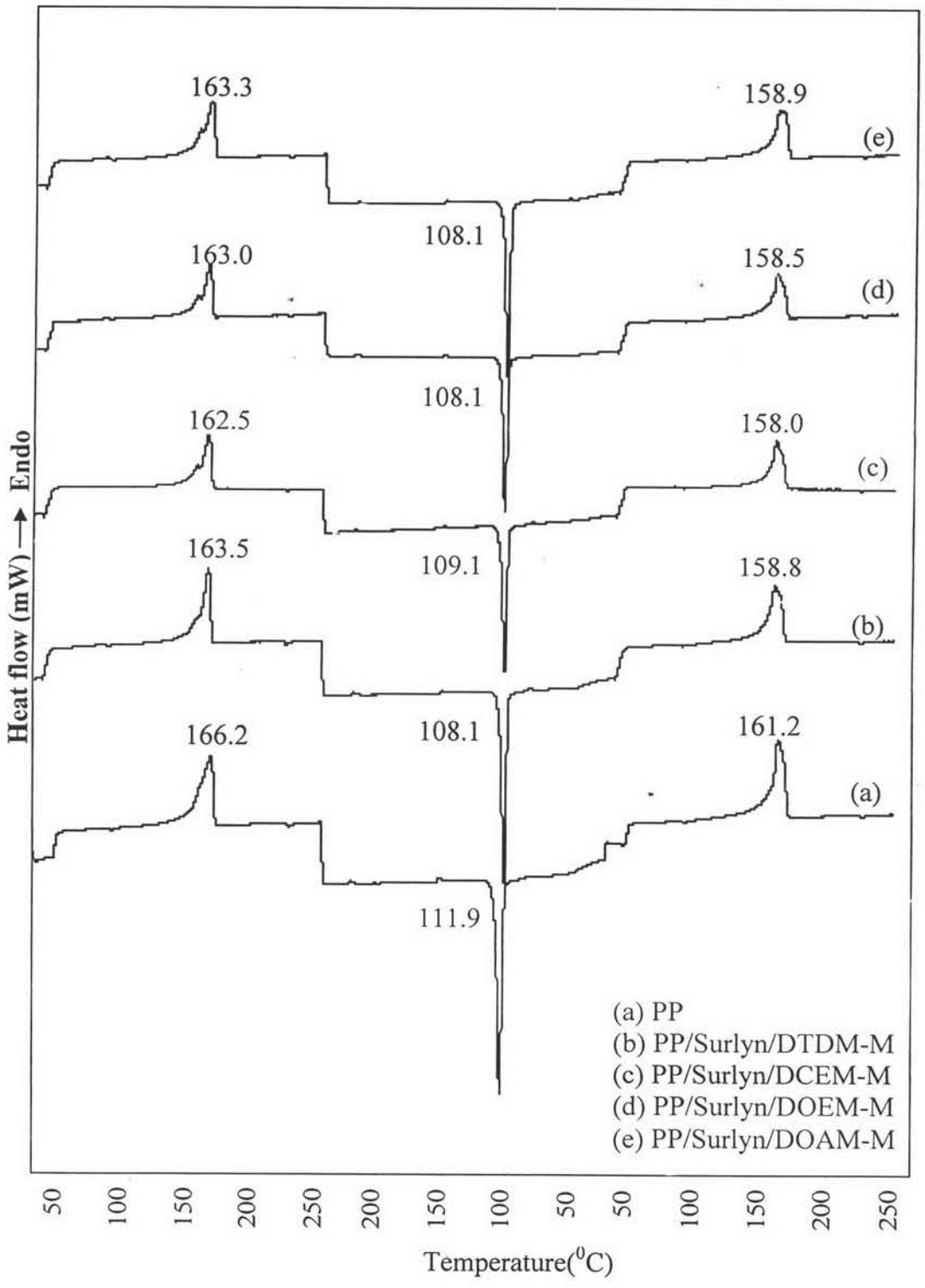

(B)

Figure 4.7 DSC thermograms of PP/Surlyn and nanocomposites formed: (A) organomodified bentonite nanocomposites, (B) organomodified montmorillonite nanocomposites.

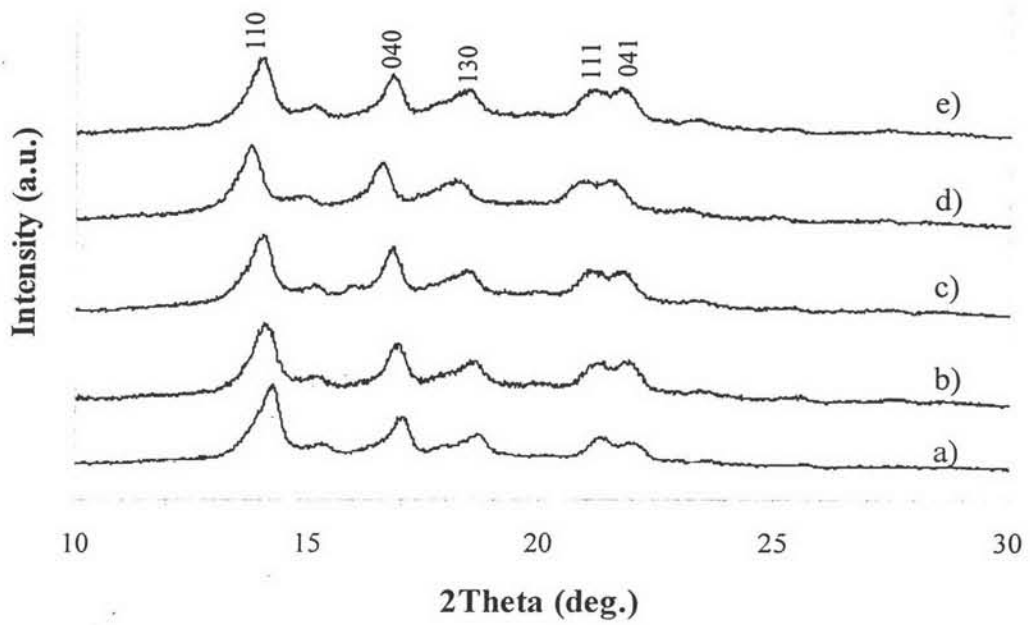

Figure 4.8 The WAXD patterns of pure PP and organomodified bentonite nanocomposites: (a) pure PP, (b) PP/Surlyn/DTDM-B, (c) PP/Surlyn/DCEM-B, (d) PP/Surlyn/DOEM-B, (e) PP/Surlyn/DOAM-B.

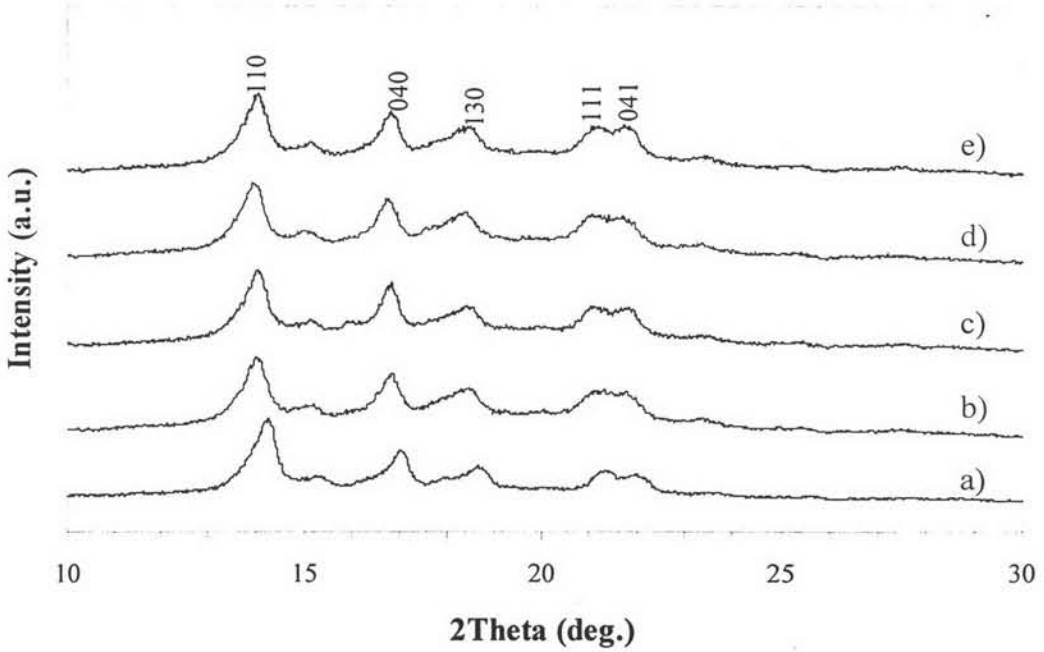

Figure 4.9 The WAXD patterns of pure PP and organomodified montmorillonite nanocomposites: (a) pure PP, (b) PP/Surlyn/DTDM-M, (c) PP/Surlyn/DCEM-M, (d) PP/Surlyn/DOEM-M, (e) PP/Surlyn/DOAM-M.

4.3.3 Thermal Properties

Fig.4.10 and Fig.4.11 show the TG and DTA curves for PP/modified bentonite nanocomposites and PP/ modified montmorillonite nanocomposites. The actual clay content and the thermal decomposition temperatures of obtained nanocomposites are listed in Table 4.6. All PP/ clay nanocomposites show overall higher thermal stability (456-459°C and 459-461°C for montmorillonite and bentonite, respectively) when compared to the virgin PP (~456°C) and PP/ Surlyn (~453°C). This is similar to the results reported by Tang *et al.* (2003). The increase thermal degradation temperature of nanocomposites is likely to be due to the present of the silicate layers on the surface of the nanocomposites creating a physical protective barrier on the surface of the material. For the nanocomposites with the various intercalation agents modified bentonite, PP/Surlyn/DCEM-B nanocomposits is higher the thermal stability than PP/Surlyn/DTDM-B nanocomposits. This might be due to the better dispersion of DCEM-B in the composites than DTDM-B, owing to the greater spacing of DCEM-B organoclay would be an advantage of the intercalation of Surlyn or PP (cf. Table 4.2). PP/Surlyn/DOAM-B nanocomposits shows lower the thermal stability than PP/Surlyn/DOEM-B nanocomposits because of the poor dispersion of DOAM-B organoclay (cf. Table 4.2). This trend is also observed in nanocomposites of montmorillonite modified with the various intercalation agents. From Table 4.6, it is shown that the actual clay content of PP/ modified montmorillonite composites are lower than PP/ modified bentonite nanocomposites to result in all of PP/ modified montmorillonite nanocomposites are slightly lower thermal stability.

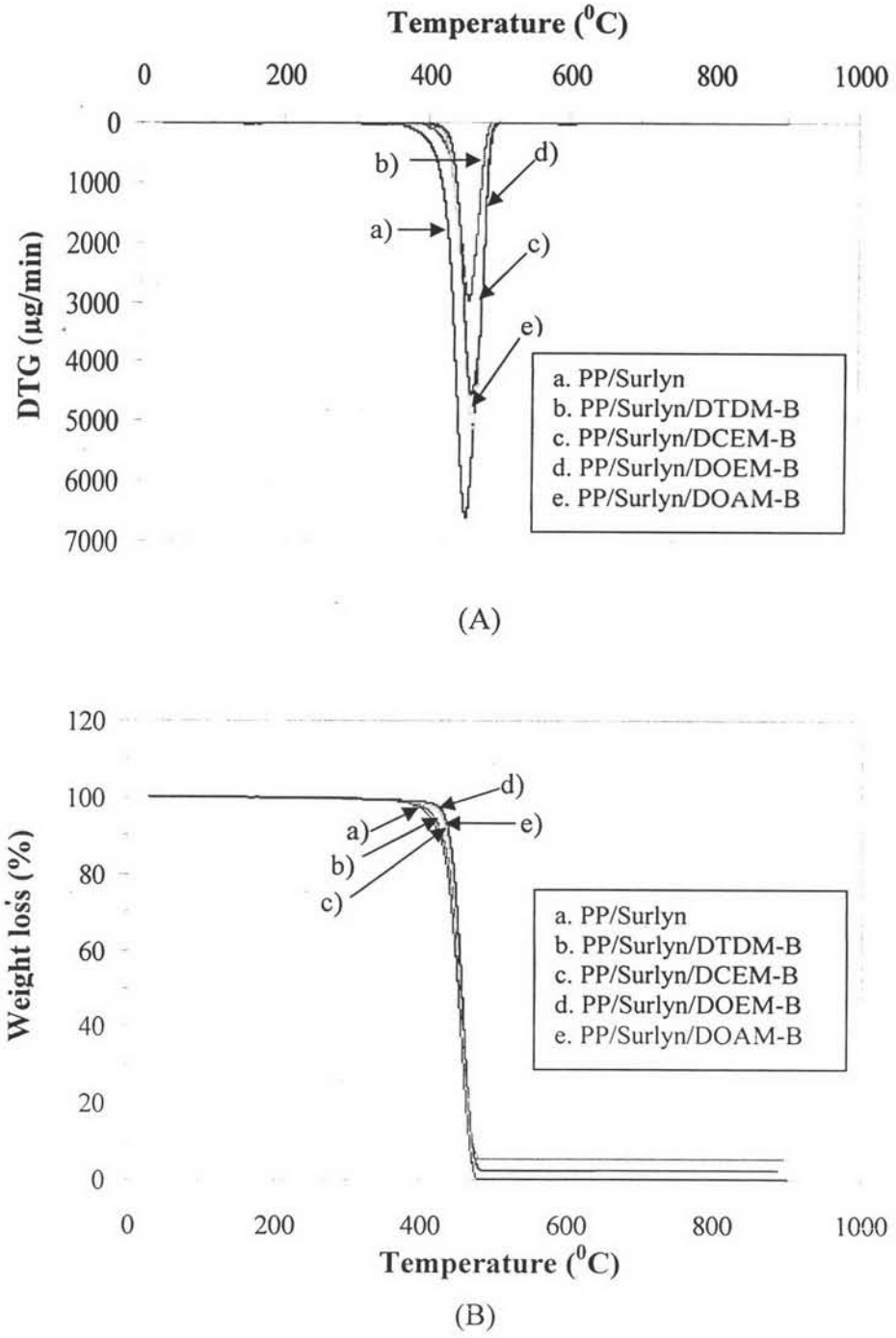

Figure 4.10 TG-DTA curves of the PP/Surlyn and organomodified bentonite nano-composites: (A) differential weight loss curves (DTG) (B) weight losses of the samples.

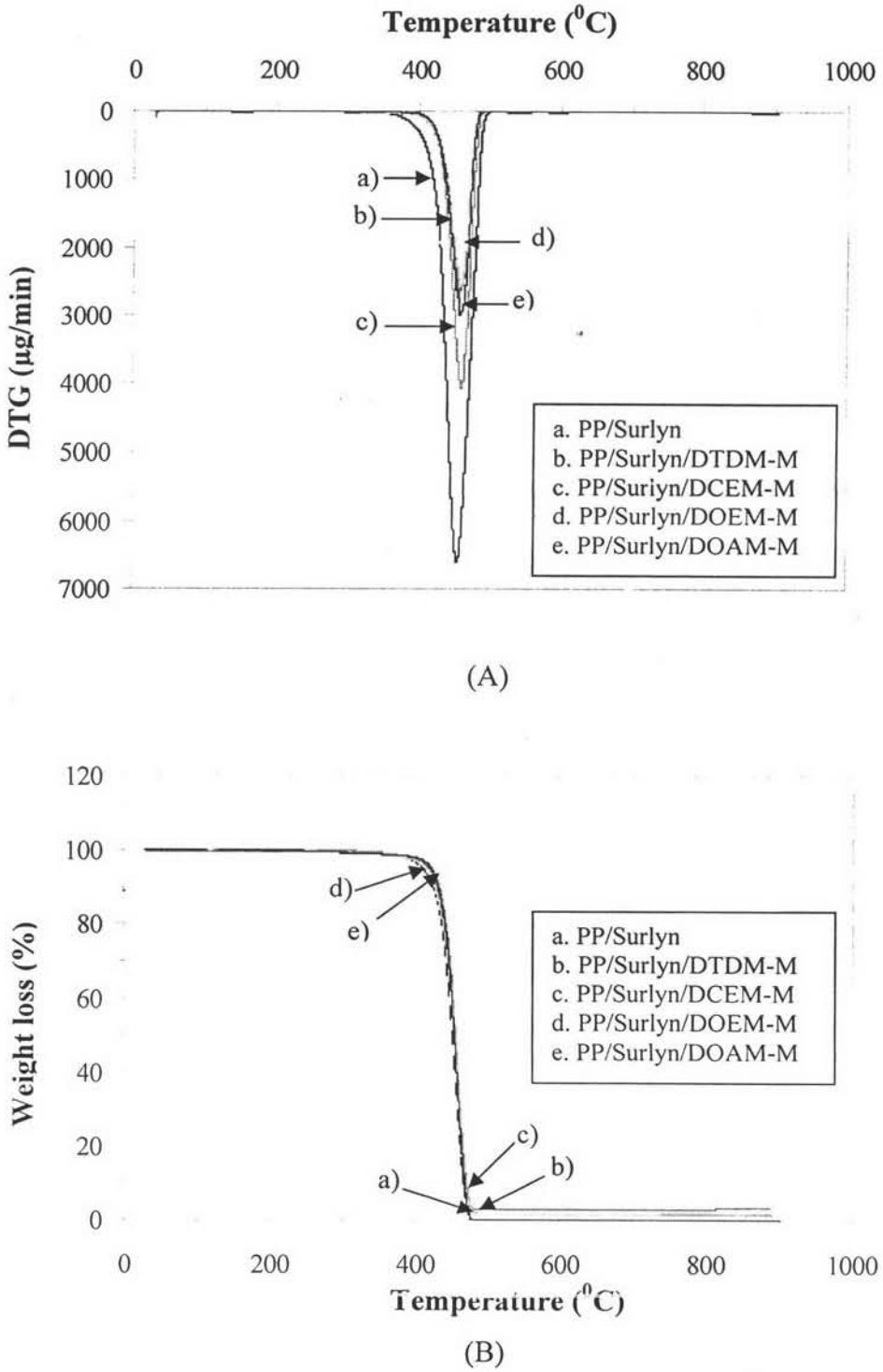

Figure 4.11 TG-DTA curves of the PP/Surlyn and organomodified montmorillonite nanocomposites: (A) differential weight loss curves (DTG) (B) weight losses of the samples.

Table 4.6 Thermal behaviors of PP and nanocomposites formed

Composition	TGA			
	Clay content (wt%)	T_d (^{0}C)	T_i (^{0}C)	T_f (^{0}C)
PP	-	455.8	432.1	468.4
PP + Surlyn	-	453.1	426.9	468.1
PP + Surlyn + DTDM-B	2.1	459.4	437.8	470.9
PP + Surlyn + DCEM-B	2.2	461.1	439.0	471.2
PP + Surlyn + DOEM-B	2.4	460.3	440.5	471.2
PP + Surlyn + DOAM-B	2.3	459.2	442.4	472.9
PP + Surlyn + DTDM-M	2.2	455.5	434.6	470.5
PP + Surlyn + DCEM-M	1.6	458.6	434.7	470.4
PP + Surlyn + DOEM-M	1.9	457.9	434.4	471.8
PP + Surlyn + DOAM-M	1.7	457.5	436.5	472.3

4.3.4 Mechanical Properties

Mechanical properties are measured in order to verify the superior characteristics of nanoscale dispersion of silicate clay layer in the PP matrix. In this work, mechanical properties of PP/modified bentonite composites are compared with PP/Surlyn and PP/modified montmorillonite composites, specifically Young's modulus, tensile strength, strain at break and notched Izod impact strength. The analysis of the trends on mechanical properties gives information about the effect of both intercalation agent and clay.

Fig. 4.12 shows young's modulus of the PP/Surlyn, PP/modified bentonite and PP/modified montmorillonite composites with various intercalation agents. All of composites give higher modulus in comparison to PP/Surlyn. Young's

modulus of organomodified bentonite composites and organomodified montmorillonite composites shows slightly lower performance in all cases. Similar results were found in PP/ clay nanocompposites prepard with two different types of clay, bentonite and commercial montmorillonite, by García-López *et al.* (2003). This different in mechanical performance might be due to the modified bentonite is low purity clay, which has many inhomogeneous aggregates of calcium impurity. For the composites of bentonite modified with the various intercalation agents and comparing the nanocomposites of bentonite modified with DTDM and DCEM, the functional groups of the intercalation agents DCEM do not effect to mechanical performance of the obtained composite. It is also observed in the composites of montmorillonite modified with DTDM and DCEM. PP/Surlyn/DOEM-B nanocomposits shows higher modulus than PP/Surlyn/DOAM-B nanocomposits due to the better dispersion of DOEM-B organoclay in the composites than DTDM-B. (cf. Table 4.1).

Tensile strength of the PP/ Surlyn, PP/ modified bentonite and PP/ modified montmorillonite composites with various intercalation agents are represent in Fig. 4.13. PP/ Surlyn/ DTDM-B nanocomposits have slightly higher tensile strength than PP/ Surlyn and other type of intercalation agents modified bentonite in the nanocomposites. This trend is also found in the PP/ modified montmorillonite composites. This would tend to suggest that the decreasing in tensile strength of nanocomposites modified with surfactant having functional group is due to incomplete pulling of chains from crystalline region (cf. Table 4.5). When it was pulling, the order structure or crystalline structure was changed and could not repack to the tensile direction therefore it cannot be pulled any further and would then break with lower strength. As show in Fig. 4.14. that by adding organoclay, the percentage of strain at break tended to decrease.

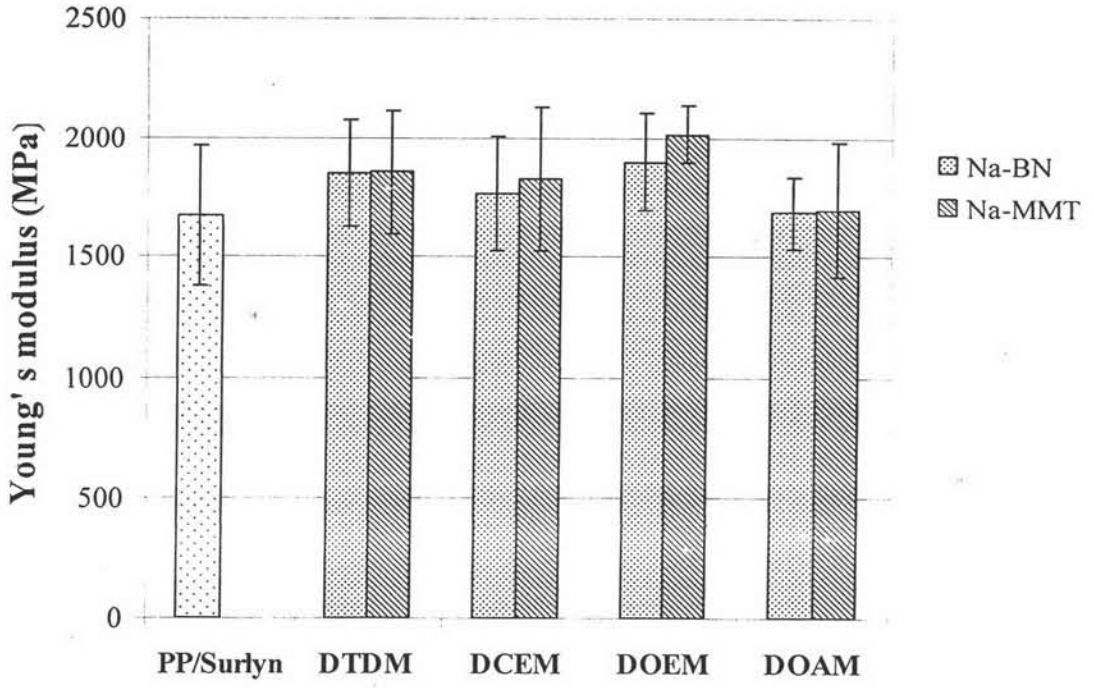

Figure 4.12 Young's modulus of the PP/Surlyn, PP/Surlyn/modified bentonite and PP/Surlyn/modified montmorillonite composites with various intercalation agents.

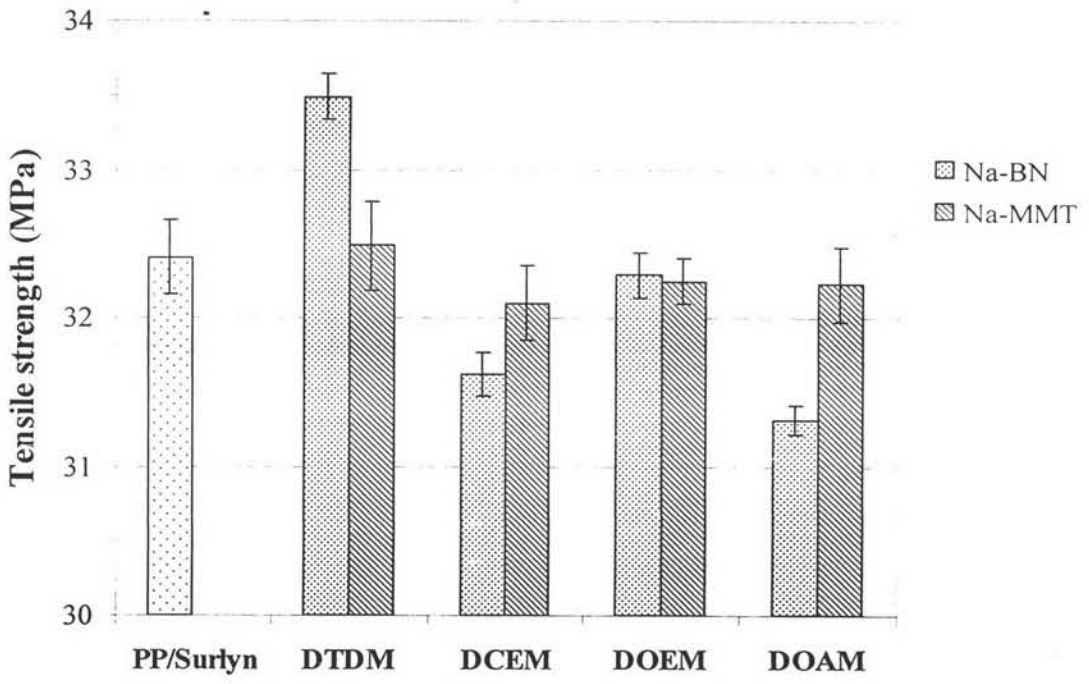

Figure 4.13 Tensile strength of the PP/Surlyn, PP/Surlyn/modified bentonite and PP/Surlyn/modified montmorillonite composites with various intercalation agents.

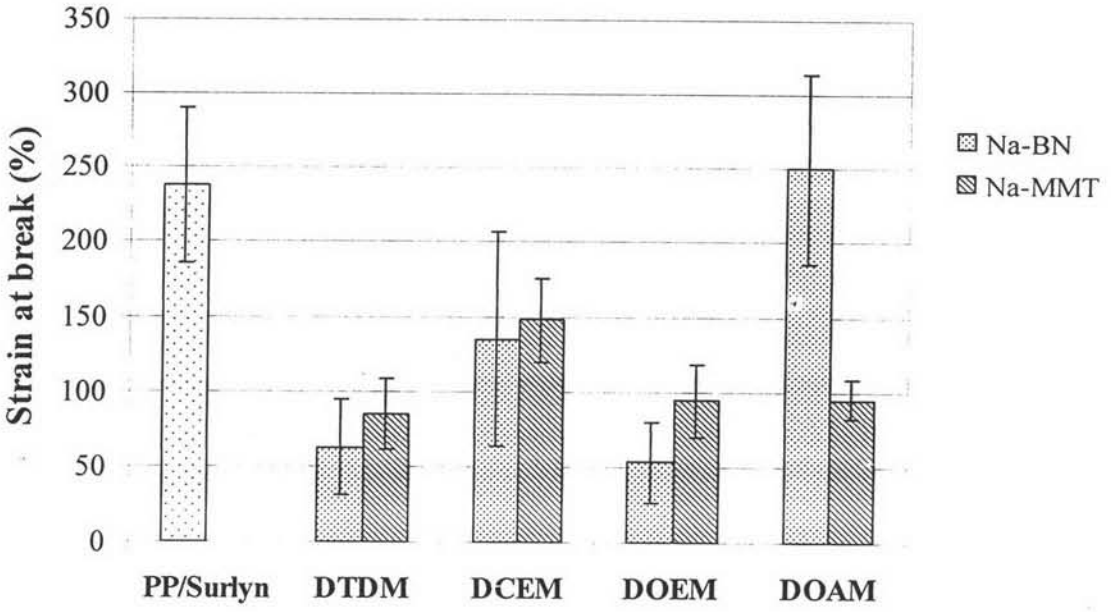

Figure 4.14 Strain at break (%) of the PP/Surlyn, PP/Surlyn/modified bentonite and PP/Surlyn/modified montmorillonite composites with various intercalation agents.

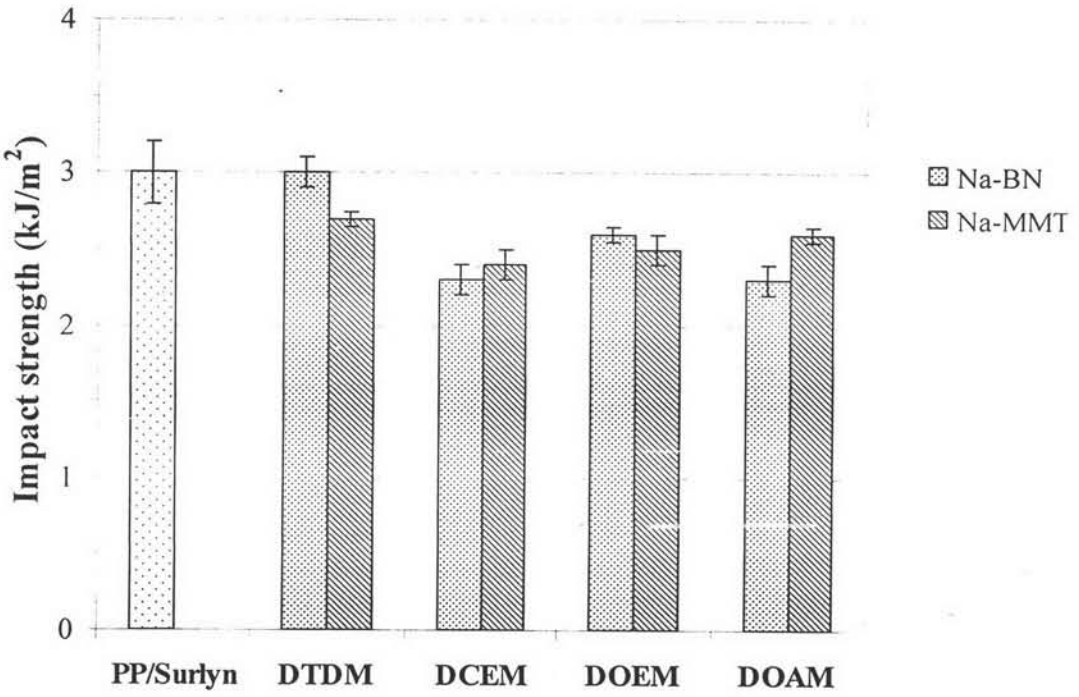

Figure 4.15 Impact strength of the PP/Surlyn, PP/Surlyn/modified bentonite and PP/Surlyn/modified montmorillonite composites with various intercalation agents.

Fig. 4.14 shows strain at break of the PP/ Surlyn, PP/ modified bentonite and PP/ modified montmorillonite nanocomposites with various intercalation agents. All of nanocomposites give lower strain at break in comparison to PP/ Surlyn due to it has the highest %crystallinity (cf. Table 4.5), as observed in the previous paper (Hasegawa *et al.*, 1998) for PP/ clay nanocomposites. For the nanocomposites of bentonite modified with the various intercalation agents, DCEM modified bentonite nanocomposites has higher strain at break than DTDM modified bentonite nanocomposites. This might be due to DCEM modified bentonite nanocomposites give higer %crystallinity (cf. Table 4.5). PP/ Surlyn/ DOEM-B nanocomposits shows higher strain at break than PP/ Surlyn/ DOAM-B nanocomposits. It is also observed the same tendency in the nanocomposites of modified montmorillonite.

Notched Izod impact strength values are in general less than that of PP/ Surlyn (as shown in Fig. 4.15). For the composites of bentonite modified with the various intercalation agents, DTDM-B organoclay in nanocomposits gives higher impact strength than the other type of orgonoclay. However, it is lower than PP/ Surlyn. One possible reason is owing to higher degree of crystallinity of nanocomposite, which did not allow absorbed energy to transfer from one phase to another phase.